

Dynamically Generated Double Occupancy as a Probe of Cold Atom Systems

S.D. Huber and A. Rüegg

Theoretische Physik, ETH Zurich, CH-8093 Zürich, Switzerland

(Dated: November 21, 2018)

The experimental investigation of quantum phases in optical lattice systems provides major challenges. Recently, dynamical generation of double occupancy via modulation of the hopping amplitude t has been used to characterize the strongly correlated phase of fermionic atoms. Here, we want to validate this experimental technique with a theoretical study of the driven Hubbard model using analytic methods. We find that conclusive evidence for a Mott phase can be inferred from such a measurement, provided that sufficiently low temperatures $k_B T \ll t$ can be reached.

PACS numbers: 03.75.Ss, 71.10.Fd, 31.15.aq

The recent progress in cooling and manipulating cold fermionic gases in optical lattices allows us to investigate phenomena at ever lower temperatures, where intriguing many-body effects generate new (quantum) phases which are of much interest in condensed matter systems as well. While the high tunability of atoms in optical lattices is a landmark advantage of these systems, the availability of methods allowing for their proper characterization lags behind the sophistication reached in solid state physics. This lack in available experimental probes gains importance, now that an increasingly larger class of non-trivial quantum phases are in reach. Their definitive identification requires the translation of the defining properties, usually expressed in terms of thermodynamic and transport coefficients, to the probes available for cold atomic systems. Recently two experiments addressed the question of strongly correlated fermions in an optical lattice [1, 2]. Schneider *et al.* [2] concentrate on the compressibility [3], while Jördens *et al.* [1] have made use of a new probe, the dynamically generated double occupancy (DGDO) proposed by Kollath *et al.* [4], in order to identify a Mott insulator state of strongly repulsive fermionic ^{40}K atoms. This technique, where the signal is the change in double occupancy after dynamical modulation of the hopping amplitude t , represents a prime example of a measurement without analog in classical solid state physics [5]. Using different analytic methods in separate regions of the parameter space, cf. Fig. 1, this Letter aims at a theoretical characterization of the DGDO scheme and its suitability to describe the transition or crossover to the fermionic Mott-insulator.

Ultracold fermions in an optical lattice are well described by the Hubbard model

$$H = -t \sum_{\langle i,j \rangle, \sigma} (c_{i\sigma}^\dagger c_{j\sigma} + \text{h.c.}) + U \sum_i D_i = -tK + UH_{\text{int}}, \quad (1)$$

where the spin degrees of freedom are realized by two hyperfine states. Here, $c_{i\sigma}^\dagger$ are fermionic operators creating particles with spin σ in a Wannier state at site i , $D_i = n_{i\uparrow}n_{i\downarrow}$ measures the double occupancy at site i , and the sum $\langle i, j \rangle$ runs over nearest neighbors for all N lattice sites. Although the phase diagram for the three

dimensional system is not precisely known yet, the qualitative form was determined (c.f. [6, 7] and references therein). In particular, at half-filling on a cubic lattice, an anti-ferromagnetic phase below $T \lesssim T_{\text{Néel}} \leq 0.3 T_F$ is expected; whereas in strongly frustrated systems, typical estimates limit the temperature for (paramagnetic) Mott physics to a regime below $0.1 T_F$ (T_F denotes the Fermi temperature).

The two defining properties of a fermionic Mott insulator are the interaction-induced incompressibility and a vanishing Drude-weight in the optical conductivity [6]. While the first is related to a gap $\Delta\mu$ in the charge spectrum and can be used as a probe in the cold atom setup as well, the measurement of the second one, relying on transport properties, is more difficult to perform. From this viewpoint, the implementation of the Hubbard Hamiltonian with cold atoms not only allows us to study this unsolved model in a controlled environment but also poses inherently new questions. In comparing theoretical and experimental results, it is of interest to know which features in the calculation (which is based on a uniform system) survive the translation to the (inhomogeneous) experimental setup. We thus characterize the DGDO technique in a wide parameter regime and conclude that frequency-integrated and bond-averaged quantities capture the desired information with the least obstructions due to confinement-induced changes of line shapes.

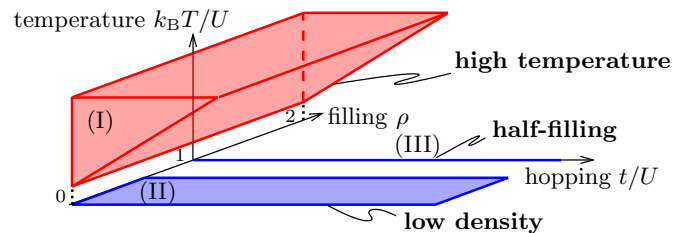


FIG. 1: (color online) Regimes where the dynamically generated double occupancy probe is analyzed: High temperatures (I) are discussed in the atomic limit. The regime at zero temperature and low densities (II) involves the solution of a two-particle problem; the situation at half filling and $T = 0$ (III) is done within a slave-spin mean-field analysis.

Our theoretical analysis of the DGDO technique involves exactly solvable limiting cases of the Hamiltonian (1), namely, the atomic limit ($t = 0$) and the two-particle problem, see Fig. 1, with results relevant in the regimes $U, T \gg t$, as well as for filling $\rho \ll 1$ (we set $k_B = 1$). On the other hand, in order to discuss the Mott physics within the DGDO technique at low temperatures, cf. Fig. 1(III), we introduce and apply a slave-spin mean-field approximation which captures the most relevant physics on both the t and U scale. Our results for the DGDO signal are summarized in Fig. 2.

We first derive the expression for the second-order response function describing the DGDO $\delta\mathcal{D}$; exciting the system during the time $\Delta\tau_{\text{mod}}$ through a (isotropic) modulation $H_{\text{mod}} = \delta t \cos(\omega\tau)K$ of the hopping amplitude, the task is to calculate the expectation value

$$\delta D(\tau) = \langle \psi(\tau) | \sum_i D_i | \psi(\tau) \rangle - \langle 0 | \sum_i D_i | 0 \rangle, \quad (2)$$

of the double-occupancy operator, where $|0\rangle$ denotes the unperturbed ground state. We write the perturbed wave function $|\psi(\tau)\rangle = \exp(iH\tau/\hbar)T_\tau \exp[-(i/\hbar) \int_{-\infty}^{\tau} d\tau' H_{\text{mod}}(\tau')] |0\rangle$, where T_τ denotes time ordering. Expanding (2) to second order in the hopping modulation δt and keeping only non-oscillatory terms $\delta D(\tau) = \pi\delta t^2 \delta\mathcal{D}(\omega) \Delta\tau_{\text{mod}}/2\hbar^2 +$

osc. $+ O(\delta t^3)$, we arrive at the spectral transition rate (the time-averaged first-order response vanishes)

$$\delta\mathcal{D}(\omega) = \sum_n \langle n | \delta D | n \rangle |\langle n | K | 0 \rangle|^2 \delta(\omega - \omega_{n0}). \quad (3)$$

Here, $|n\rangle$ denote the excited states with energy $\hbar\omega_{n0} = \hbar\omega_n - \hbar\omega_0$. Note, that in the current experiment [1], $\delta D(\tau)$ is not $\propto \Delta\tau_{\text{mod}}$, however [8]. We define the integrated quantity

$$\delta\mathcal{D}_{\text{tot}} = \frac{2}{Nz} \int d\omega \delta\mathcal{D}(\omega), \quad (4)$$

normalized to the number $Nz/2$ of bonds in the system ($z = \text{coordination number}$). In the non-interacting limit ($U = 0$), the eigenstates of (1) are those of K and no excitations are induced, hence $\delta\mathcal{D}_{\text{tot}}$ vanishes and a finite interaction U is required to generate a finite result. In the following, we evaluate (4) in the regimes (I)–(III).

In the atomic limit ($t = 0$, region I), the calculation of the *change* in the double occupancy reduces to a two-site problem and $\delta\mathcal{D}_{\text{tot}}$ is given by the square of the probability to find a singly occupied lattice site; its rapid increase signals the crossover from weak to strong correlations. In the limit $U \gg T$, $\delta\mathcal{D}_{\text{tot}}$ saturates at ρ^2 for $\rho \leq 1$ and at $(2 - \rho)^2$ for $\rho \geq 1$ [cf. Fig. 2(a)]. The atomic limit, valid in the regime $U, T \gg t$, offers a good starting point for analyzing current experiments [1, 3].

In the low density limit ($\rho < 1$, region II), we analyze the DGDO by exactly solving the two-particle problem with Hubbard interaction [9, 10]. One then expects a signature at finite frequency of order U , as two fermions (in a singlet state) on the same site cost an energy U , irrespective of the density. We only consider the $d = 1$ -dimensional case here, the extension to higher dimensions is straightforward. The two-particle wave function in the singlet channel, $\psi_{\text{scat}}(r) = \langle r | k_1, k_2 \rangle_{\text{scat}}$, with r the relative coordinate and k_1 and k_2 the momenta of the two atoms, can be obtained by solving the Lippmann-Schwinger equation (we ignore the center of mass motion). Expanding the solution $\psi_{\text{scat}}(r)$ in Bloch waves $\psi_{\text{Bloch}}(r) = \langle r | k_1, k_2 \rangle_{\text{Bloch}}$ we find the amplitudes

$$\langle q, k' | q, k \rangle_{\text{scat}} = \delta_{k, k'} + \frac{(U/N)f(q, k)}{\epsilon_{q, k} - \epsilon_{q, k'} + i\eta}, \quad (5)$$

with $\epsilon_{k, q} = 4t \cos(q) \cos(k/2)$ the bare dispersion and $f(q, k) = [1 + U/4ti |\sin(k/2) \cos(q)|]^{-1}$ the scattering amplitude. Here, $q = (k_1 + k_2)/2$ and $k = k_1 - k_2$ are the total and relative momenta of the two atoms. In addition, a bound state $\psi_{\text{bs}}(r)$ with amplitudes

$$\langle q, k' | q \rangle_{\text{bs}} = (2U^3/\epsilon_q^{\text{bs}})^{1/2} / (\epsilon_{q, k'} - \epsilon_q^{\text{bs}}) \quad (6)$$

and energy $\epsilon_q^{\text{bs}} = \sqrt{U^2 + [4t \cos(q)]^2}$ is found. Rewriting $K = (H_{\text{int}} - H)/t$ with $H_{\text{int}} = U\delta_{r,0}$, we find for the total DGDO (4) per singlet pair $\{k_1, k_2\}$,

$$\delta\mathcal{D}_{\text{tot}}^{k_1, k_2} = [\psi_{\text{bs}}^2(0) - \psi_{\text{scat}}^2(0)](U/t)^2 \psi_{\text{bs}}^2(0) \psi_{\text{scat}}^2(0); \quad (7)$$

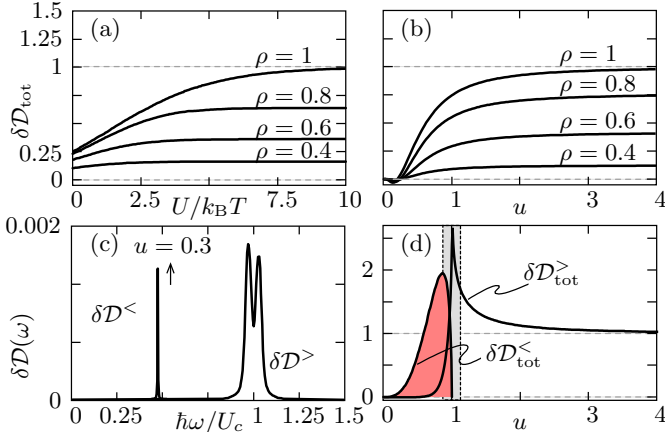


FIG. 2: (color online) Characteristic DGDO signal for the different regimes (I)–(III) of Fig. 1. (a) For the high temperature region (I), we find an increase in $\delta\mathcal{D}_{\text{tot}}$ for increasing U/T and a saturation value $\delta\mathcal{D}_{\text{tot}} \rightarrow \rho^2$ at $U \gg T$. (b) For the low density phase at $T = 0$, we find the same behavior with a saturating response at $u = U/U_c \gg 1$ where $\delta\mathcal{D}_{\text{tot}} \rightarrow \rho^2[1 - \sin(4\pi\rho)/4\pi\rho]$. The response of the system at half-filling and $T = 0$ (III) changes its behavior significantly at $u = 1$. (c) Spectral DGDO signal $\delta\mathcal{D}(\omega)$ with peaks at $\hbar\omega = \Delta$ and around $\hbar\omega \approx \max(U_c, U)$ identifying transitions between the Gutzwiller and upper Hubbard- and those between the lower and higher Hubbard bands, respectively. (d) Total weights $\delta\mathcal{D}_{\text{tot}}^{<}$ accumulated in the two peaks in (c). Shown in grey is the fluctuation region $|u - 1| < u^{\text{fl}}$ where our mean-field analysis is not valid.

the above result originates from process where two particles in the scattering state $|q, k\rangle_{\text{scat}}$ combine to a repulsively bound pair $|q\rangle_{\text{bs}}$. To obtain the full result at small but finite density ρ , we have to calculate $\delta\mathcal{D}_{\text{tot}} = \sum_{k_1, k_2} n_{k_1, k_2} \delta\mathcal{D}_{\text{tot}}^{k_1, k_2}$, where n_{k_1, k_2} is the ground state expectation value to find a pair $\{k_1, k_2\}$ in the singlet channel, see Ref. [9]. The final result, cf. Fig. 2(b), shows again an increasing signal for small U/t and a saturation at large U/t , with $\delta\mathcal{D}_{\text{tot}} \rightarrow \rho^2[1 - \sin(4\pi\rho)/4\pi\rho]$. While the derivation assumes low density, the result up to $\rho = 1$ are shown for comparison with the other approaches [9].

We now turn to the low-temperature regime of the half-filled Hubbard model (1) in three dimensions, the region III in Fig. 1. Depending on the amount of Fermi-surface nesting, an anti-ferromagnetic phase intervenes with the Mott physics. For the optical lattice implementation this would require an initial cooling to about $T_i \approx 0.02 T_F$ [7]. Within the slave-spin mean-field treatment used here, the possibility for the appearance of such a magnetic order is ignored. All our results below can be obtained within the four-boson approach of Kotliar and Ruckenstein [11] which builds on earlier slave-boson methods [12, 13]. However, we apply a minimal formalism reminiscent of the slave-spin [14] or the slave-rotor formulation [15] which captures all aspects relevant to our present discussion.

On each lattice site, we introduce an auxiliary pseudospin-1/2 \mathbf{S} with eigenstates (of S_z) $|+\rangle$ ($|-\rangle$) encoding double and empty (singly) occupied sites with excitation energies of order U . In addition, auxiliary fermionic operators f_σ are introduced to describe the low-energy quasiparticle degrees of freedom. The physical creation (annihilation) operators of the original model then are represented as $c_\sigma^{(\dagger)} = 2S^x f_\sigma^{(\dagger)}$. The physical states in the enlarged Hilbert-space are $|e\rangle = |+, 0\rangle$, $|d\rangle = f_\uparrow^\dagger f_\downarrow^\dagger |+, 0\rangle$, $|\uparrow\rangle = f_\uparrow^\dagger |-, 0\rangle$, and $|\downarrow\rangle = f_\downarrow^\dagger |-, 0\rangle$, where $|0\rangle$ is the vacuum of the f -fermions. The projection onto the physical subspace is achieved by imposing for each site i the constraint $S_i^z + 1/2 = (\sum_\sigma f_{i\sigma}^\dagger f_{i\sigma} - 1)^2$; as a result, H_{int} involves solely pseudospin operators S_i^z .

Within our mean-field solution, we assume product states in pseudo spin and fermion degrees of freedom, thereby relaxing the above constraint. Within this approximation, the canonical anti-commutation relations are preserved on average, $\langle\{c_{i\sigma}, c_{j\sigma'}^\dagger\}\rangle = 4\langle S_i^x S_j^x \rangle \langle\{f_{i\sigma}, f_{j\sigma'}^\dagger\}\rangle = \delta_{\sigma\sigma'} \delta_{ij}$, where $\langle\ldots\rangle$ denotes the average over mean-field eigenstates. As a consequence, the single-particle spectral weight is preserved as long as the spin identity $(S_i^x)^2 \equiv 1/4$ is respected.

We obtain two effective mean-field Hamiltonians: The fermion problem assumes the form of a non-interacting tight-binding Hamiltonian with a hopping amplitude renormalized by a factor $g_{ij} = 4\langle S_i^x S_j^x \rangle$, with i, j nearest neighbors. On the other hand, the pseudospin problem

reduces to the transverse Ising model

$$H_{\text{TIM}} = - \sum_{\langle i, j \rangle} J_{ij} S_i^x S_j^x + h \sum_i S_i^z, \quad (8)$$

with the transverse field $h = U/2$ and the exchange coupling $J_{ij} = 4t \sum_\sigma (\langle f_{i\sigma}^\dagger f_{j\sigma} \rangle + \text{c.c.})$. The transverse Ising model is a prime example of a system displaying a quantum critical point at a critical ratio $(2h/J)_c = (U/J)_c$, separating a magnetically ordered phase from a quantum paramagnet. In the following, we restrict our analysis to translation-invariant states, for which $J_{ij} = J = -(16/z) \int_{-2td}^0 d\varepsilon \varepsilon \rho_\sigma(\varepsilon) \approx 2.67t$, and $\rho_\sigma(\varepsilon)$ is the non-interacting density of states per spin.

Applying a single-site molecular-field approximation to Eq. (8), the critical ratio is given by $(U/J)_c = z$ and we recover the result of the Gutzwiller approximation [16] of the Hubbard model. Within the molecular-field approximation, the magnetization of the pseudospin points along the z -component of the quantization axis rotated around the y -axis due to the action of the magnetic field h (or interaction U). The angle of rotation is given by $\tan(\varphi) = \sqrt{1 - u^2}/u$ for $u \leq 1$ and $\tan(\varphi) = 0$ for $u > 1$, where $u = U/U_c$. The fluctuations around this magnetization are calculated within a spin-wave analysis [17, 18] and we find the gapped pseudospin-wave spectrum

$$\hbar\omega(\mathbf{k}) = \frac{U_c}{2} \times \begin{cases} \sqrt{1 + \gamma_{\mathbf{k}} u^2}, & \text{for } u \leq 1, \\ \sqrt{u^2 + \gamma_{\mathbf{k}} u}, & \text{for } u > 1, \end{cases} \quad (9)$$

with $\gamma_{\mathbf{k}} = -(1/d) \sum_{i=1}^d \cos(k_i)$ and an excitation gap $\Delta = \hbar\omega(0)$.

The quantum criticality at $u = 1$ is reflected in the softening of the mode (9). For $u > 1$, the jump $\Delta\mu$ in the chemical potential from hole to particle doping amounts to twice the excitation gap, $\Delta\mu = 2\Delta$; the above

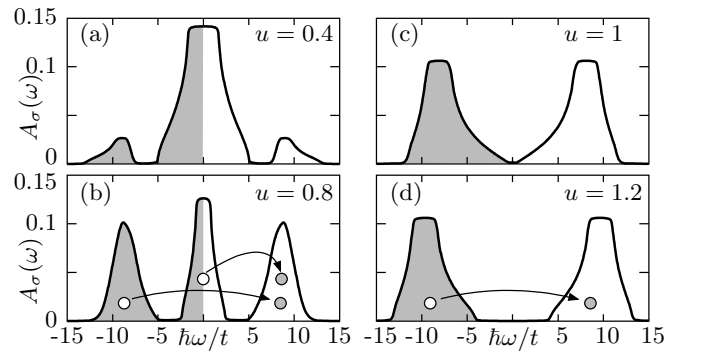


FIG. 3: The single-particle spectral density (per spin σ) $A_\sigma(\omega)$ calculated within the slave-spin theory for different interaction strengths u . In the metallic phase, panels (a) and (b), the DGDO probe can induce transitions to the upper Hubbard band from either the coherent Gutzwiller band at $\hbar\omega = 0$ or the lower Hubbard band, see (b). In the insulating state, only the latter possibility remains, see (d).

pseudospin-mode corresponds to the gapped charge excitation of the Mott insulator [19, 20].

To estimate the validity of the molecular-field plus spin-wave calculation, we compare fluctuations with the magnitude of the order parameter and define u^n through the condition $1/(z+1)[\sum_{\langle 0,i \rangle} \langle \delta S_0^x \delta S_i^x \rangle + \langle (\delta S_0^x)^2 \rangle] = \langle S_0^x \rangle^2|_{u^n}$. For the cubic lattice, we obtain $u^n \approx 0.9$, hence, for $u \approx 1 \pm 0.1$ the fluctuation induced corrections to the molecular-field result are important and the validity of the above analysis is limited.

Below, we will see that the DGDO can be qualitatively understood by the structure of the single-particle spectral density, which is defined as $A_\sigma(\omega) = -\sum_{\mathbf{k}} \text{Im} G_\sigma^R(\mathbf{k}, \omega)/N\pi$. Here, $G_\sigma^R(\mathbf{k}, \omega)$ is the retarded single-particle Green's function of the c -fermions which is calculated in a straightforward way using the Lehmann representation. The result is shown in Fig. 3 in the metallic as well as in the insulating phase. The gapped mode found in the transverse Ising model leads to the *incoherent* weight around $\pm \max(U_c, U)/2$ in the spectral density. In the metallic phase, we find the characteristic three peak structure with preformed Hubbard bands centered at $\hbar\omega \approx \pm U_c/2$ and a coherent Gutzwiller band at $\hbar\omega \approx 0$. The Gutzwiller band disappears at $u = 1$ and the Hubbard bands touch at $\hbar\omega = 0$. For $u \gg 1$ the Hubbard bands assume a constant width of $U_c/2$ and are separated by U . The approximate nature of our treatment of the spin problem violates $\langle S_i^x \rangle^2 \equiv 1/4$ and the spectral weight fails to be properly normalized. This failure only manifests itself in the fluctuation regime, however.

The nonlinear DGDO signal is calculated from Eq. (3) by expressing H_{int} and K in terms of the slave-spin operators; a careful analysis of the consistency in the order of expansion is crucial. For $u \leq 1$, we find *two* distinct features in $\delta\mathcal{D}(\omega)$, cf. Fig. 2: The sharp peak at $\hbar\omega = \Delta$ with weight $\delta\mathcal{D}_{\text{tot}}^<$ is due to the excitation of a pseudospin-wave mode at $\mathbf{k} = 0$. In the fermionic language, this corresponds to the process where the system is excited from the Gutzwiller band to the upper Hubbard band, cf. Fig. 3(b). The peak measures the quasiparticle weight Z , which is absent in the insulating state; hence its vanishing serves as a clear signal for the metal-insulator transition. Without the inclusion of quasiparticle interactions, the peak is infinitely sharp. The broad peak around $\hbar\omega \approx \max(U_c, U)$ with weight $\delta\mathcal{D}_{\text{tot}}^>$ originates from a continuum of pairs of pseudospin waves and corresponds to the excitation across the gap between the (preformed) upper and lower Hubbard bands, cf. Fig. 3(d); this feature survives the phase transition and $\delta\mathcal{D}_{\text{tot}}^>$ saturates at $u \gg 1$. The double-peak structure in Fig. 2 is an artifact of our mean-field approach [18]. To obtain the exact line-shape a more complicated calculation is required.

In conclusion, we have calculated the DGDO in various regimes and have investigated the suitability of this probe to characterize the Mott transition in a fermionic system. To make the closest contact to experiment we find that

it is convenient to study the integrated weight $\delta\mathcal{D}_{\text{tot}}$.

For a characterization of the localized phase our findings show that the weight $\delta\mathcal{D}_{\text{tot}}^>$ from frequencies $\hbar\omega \approx U$ is not an optimal measure for Mott physics: All regimes, low density, high temperatures (single-site problem), as well as the half-filled case display qualitative similar results. Only a quantitative analysis allows to distinguish different regimes: the DGDO signal $\delta\mathcal{D}_{\text{tot}}^>$ in the interaction dominated regime saturates at a *density dependent* value which is largest at half filling. It turns out, however, that one can uniquely identify the Mott transition in a strongly frustrated system by making the distinction between $\delta\mathcal{D}_{\text{tot}}^<$ and $\delta\mathcal{D}_{\text{tot}}^>$. These two weights characterize the transitions between the Gutzwiller and upper Hubbard and those between the lower and higher Hubbard bands, respectively. The quantity $\delta\mathcal{D}_{\text{tot}}^<$ traces the quasiparticle weight Z and captures the presence of the coherent Gutzwiller band in the metal; its vanishing then serves as a clear signal to identify the Mott transition. The main effect of a trapping potential on the disappearance of this coherent signal is expected to come from a residual signal from the low-density regime in the periphery of the trap and its influence on the close-by insulator.

We thank the group of T. Esslinger, G. Blatter, M. Sigrist, T.M. Rice, E. Demler, D. Pekker, R. Sensarma, and L. Pollet for insightful discussions and acknowledge financial support from the Swiss National Foundation through the NCCR MaNEP.

-
- [1] R. Jördens, N. Strohmaier, K. Günter, H. Moritz, and T. Esslinger, *A Mott insulator of fermionic atoms in an optical lattice*, Nature **455**, 204 (2008), URL.
 - [2] U. Schneider, L. Hackermüller, S. Will, T. Best, I. Bloch, T. A. Costi, R. W. Helmes, D. Rasch, and A. Rosch, *Metallic and Insulating Phases of Repulsively Interacting Fermions in a 3D Optical Lattice*, Science **322**, 1520 (2008), URL.
 - [3] V. W. Scarola, L. Pollet, J. Oitmaa, and M. Troyer, *Discerning Incompressible and Compressible Phases of Cold Atoms in Optical Lattices*, arXiv:0809.3239v1 (2008), URL.
 - [4] C. Kollath, A. Iucci, I. P. McCulloch, and T. Giamarchi, *Modulation spectroscopy with ultracold fermions in an optical lattice*, Phys. Rev. A **74**, 041604(R) (2006), URL.
 - [5] S. Fölling, A. Widera, T. Müller, F. Gerbier, and I. Bloch, *Formation of Spatial Shell Structure in the Superfluid to Mott Insulator Transition*, Phys. Rev. Lett. **97**, 060403 (2006), URL.
 - [6] M. Imada, A. Fujimori, and Y. Tokura, *Metal-insulator transitions*, Rev. Mod. Phys. **70**, 1039 (1998), URL.
 - [7] L. De Leo, C. Kollath, A. Georges, M. Ferrero, and O. Parcollet, *Trapping and cooling fermionic atoms into the Mott and Néel states*, arXiv:0807.0790v2 (2008), URL.
 - [8] E. Demler, private communications.
 - [9] P. F. Maldague, *Optical spectrum of a Hubbard chain*,

- Phys. Rev. B **16**, 2437 (1977), URL.
- [10] K. Winkler, G. Thalhammer, F. Lang, J. Hecker Denschlag, A. J. Daley, A. Kantian, H. P. Büchler, and P. Zoller, *Repulsively bound atom pairs in an optical lattice*, Nature **441**, 853 (2006), URL.
 - [11] G. Kotliar and A. E. Ruckenstein, *New Functional Integral Approach to Strongly Correlated Fermi Systems: The Gutzwiller Approximation as a Saddle Point*, Phys. Rev. Lett. **57**, 1362 (1986), URL.
 - [12] S. E. Barnes, *New method for the Anderson model*, J. Phys. F: Met. Phys. **6**, 1375 (1976), URL.
 - [13] P. Coleman, *New approach to the mixed-valence problem*, Phys. Rev. B **29**, 3035 (1984), URL.
 - [14] L. de Medici, A. Georges, and S. Biermann, *Orbital-selective Mott transition in multiband systems: Slave-spin representation and dynamical mean-field theory*, Phys. Rev. B **72**, 205124 (2005), URL.
 - [15] S. Florens and A. Georges, *Slave-rotor mean-field theories of strongly correlated systems and the Mott transition in finite dimensions*, Phys. Rev. B **70**, 035114 (2004), URL.
 - [16] M. C. Gutzwiller, *Effect of Correlation on the Ferromagnetism of Transition Metals*, Phys. Rev. Lett. **10**, 159 (1963), URL.
 - [17] Y.-L. Wang and B. R. Cooper, *Collective Excitations and Magnetic Ordering in Materials with Singlet Crystal-Field Ground State*, Phys. Rev. **172**, 539 (1968), URL.
 - [18] S. D. Huber, E. Altman, H. P. Büchler, and G. Blatter, *Dynamical properties of ultracold bosons in an optical lattice*, Phys. Rev. B **75**, 085106 (2007), URL.
 - [19] M. Lavagna, *Functional-integral approach to strongly correlated Fermi systems: Quantum fluctuations beyond the Gutzwiller approximation*, Phys. Rev. B **41**, 142 (1990), URL.
 - [20] C. Castellani, G. Kotliar, R. Raimondi, M. Grilli, Z. Wang, and M. Rozenberg, *Collective Excitations, Photoemission Spectra, and Optical Gaps in Strongly Correlated Fermi Systems*, Phys. Rev. Lett. **69**, 2009 (1992), URL.